



Pd- and Pt-Doped Graphene Quantum Dots for SO₂ Adsorption and Dissociation: A Non-periodic DFT Study

Reza Behjatmanesh-Ardakani^{*1}, Rovnag Rzayev²

¹Department of Chemical Engineering, Faculty of Engineering, Ardakan University, P.O. Box: 184, Ardakan, Iran.

²Department of Engineering and Applied Sciences, Azerbaijan State University of Economics, UNEC, Azerbaijan

ARTICLE INFO

Article history:

Received 24 August 2024

Received in revised form 19 September 2024

Accepted 3 October 2024

Available online 4 December 2024

Keywords:

SO₂ adsorption,
SO₂ reduction, Pt-doped,
Pd-doped,
graphene quantum dot

ABSTRACT

Commonly, transition metal catalysts such as Pt and Pd are used to adsorb and dissociate SO₂ gas. Usually, SO₂ adsorption energies on these metals are in the range of -1.0 to -1.5 eV, and the barrier energies are in the range of +0.5 to +1.0 eV. These small values of barrier energies cause that SO₂ is readily converted to atomic sulfur, and the catalysts surfaces are poisoned by sulfur. In this paper, Pd- and Pt-doped graphene quantum dots are proposed as SO₂ removal catalysts from flue gas emission. SO₂ removal catalysts should have high barrier energy to prevent sulfur formation from SO₂ dissociation, but have moderate SO₂ adsorption energy to simply adsorb and desorb SO₂. Using non-periodic density functional theory, the adsorption and dissociation of SO₂ on Pd- and Pt-doped graphene quantum dots are investigated to test whether these catalysts are suitable for SO₂ removal. The data show that the adsorption energies of SO₂ on Pt- and Pd-doped graphene are in the range of -0.6 to -0.8 eV and -0.6 to -1.0 eV, respectively. However, their barrier energies are greater than +2.0 eV which is more than twice those on the transition metal surfaces. While these catalysts are good candidates for SO₂ removal, they are not suitable for SO₂ dissociation. The high barrier energies, contrary to the pristine transition metal surfaces, prevent the poisoning of the surfaces of the studied catalysts.

1. Introduction

SO₂ is an important air pollutant that can readily interact with water molecules in the air, producing acid rain. Therefore, its sensing and removal, even in small amounts, is highly desirable [1]. Commonly, transition metal surfaces such as Ni [2-4], Cu[5-8], Mo [9], Ru [10], Pt [11], and Pd [12] are used to remove SO₂ by reducing it to sulfur. Data indicate that these precious metals are capable of effectively adsorbing and dissociating SO₂, but their high costs make it essential to explore alternative, cheaper catalysts. Very recently, Kumar used oxygen-defected graphene oxide to detect low concentrations of SO₂ [13]. It seems that modified graphene has the potential to replace expensive metal catalysts in the adsorption and decomposition of SO₂.

It has been shown that pristine graphene has a low adsorption energy for the SO₂ molecule in the gas phase [14]. Luo et al. showed that the adsorption energy of SO₂

on the surface of pristine graphene is only -0.3 eV, while doping with N and Ti atoms increases the adsorption energy to -0.45 eV and -1.62 eV, respectively [15]. Dual doping of N and Ti further increases the adsorption energy of SO₂ to -2.84 eV [15]. Yan et al. used the DFT-D2 method to model the interaction of SO₂ with pristine, Co-, and Ti-doped graphene, and showed that the interaction energy of SO₂ with graphene increases from -0.65 eV for pristine to -3.63 eV and -4.63 eV, for Co- and Ti-doped graphene, respectively [16]. These studies demonstrate that modification of graphene by transition metals enhances its interaction with the SO₂ molecule.

Louis et al. modeled M-decorated Si-doped graphene (with M= Cu, Ag, and Au) to trap SO₂ gas [17]. They showed that the SO₂ adsorption energy is in the range of -0.31 eV to -1.98 eV. The complexes are thermodynamically stable, with negative ΔG and negative ΔH . Zhang et al. modeled the adsorption of SO₂ on the

* Corresponding author; e-mail: behjatmanesh@ardakan.ac.ir

<https://doi.org/10.22034/crl.2024.474971.1412>



surface of the Be, Ca, Sr, and Ba-decorated double vacancy graphene [18].

In all cases, the alkaline earth metals donate electrons to the graphene. They showed that Ba-decorated graphene adsorbs SO₂ more strongly than the other metals. There are also other theoretical studies on the adsorption of SO₂ on the surface of doped graphene [14, 19-25]. However, none of these studies provide information about the barrier energy for SO₂ dissociation. To obtain detailed information about the transition state (TS) structure and barrier energy, theoretical DFT methods are promising candidates.

DFT can help us to model new non-synthesized catalysts to predict their electronic and geometric properties [26-38]. In this paper, we utilized non-periodic DFT with a numeric basis set to investigate the adsorption and direct proportional dissociation of SO₂ on the surface of Pt- and Pd-doped graphene quantum dots. We chose Pt- and Pd-doped graphene, as literature data show that Pt and Pd pure metals are good candidates for SO₂ adsorption and dissociation with low barrier energies. Various local minima for SO₂ on the Pt- and Pd-doped graphene surface were identified, and their adsorption energies were computed. We also examined the direct dissociation of SO₂ and SO to SO + O and S + O, respectively, and estimated the reaction energies and barrier energies involved. The paper is organized as follows: we first provide details on the model used, followed by a discussion on the geometrical and electronic structure of different configurations of SO₂ adsorption on the graphene surface, and finally, we compare the dissociation energies and transition structure

2. Computational methods

A 6×6 supercell of graphene was considered to build the quantum dots Pt- and Pd-doped graphene. The periodic supercell was converted to the non-periodic one, and all dangling bonds were capped by hydrogen atoms. One of the middle carbon atoms was replaced by a Pt or Pd atom, and the catalyst was optimized using rPBE level of theory [39]. The PBE functional is a well-known GGA functional which has been used in different catalytic reaction simulations [40-44]. The optimized size of the Pt-doped graphene was 14.22 Å × 14.16 Å, and for the Pd-doped graphene, it was 14.22 Å × 14.18 Å. The optimized longest diameters of the above catalysts are approximately 2.2 nm. The optimized structures are depicted in Fig. 1. The valence electrons were represented by a double numeric + polarized (DNP) basis set, and the core electrons were modeled using a density functional semi-core pseudopotential [45]. For different configurations of

reactants, transition states, and products, the basis set superposition error (BSSE) was calculated. The maximum BSSE in this study was equal to 0.1 eV which is much smaller than the barrier energies. On the other hand, the BSSE of reactants/products and transition structures cancel each other. So, it is logical to ignore the BSSE effect on the results, and suppose that the DNP is sufficiently large for the calculations. A spin-unrestricted model was used for all calculations. For geometry optimizations, tolerances of 10⁻⁵ Ha for energy convergence, 0.002 Ha/Å for force convergence, and 0.01 Å for displacement convergence were considered. A tolerance value of 10⁻⁶ Ha was used for the SCF energy convergence. All calculations were performed using the Dmol³ code [46, 47]. Frequency analysis was done for the reactants and products to test that the structures are in the local minima in the potential energy surface.

The adsorption configurations were presented following the notation used by Jiang et al. [48]. In this notation, $\eta^i(\text{S})-\eta^j(\text{O})-\eta^k(\text{O})$ represents a configuration in which the S atom interacts directly with *i* C/Pt/Pd atoms, and the two O atoms interact with *j* and *k* C/Pt/Pd atoms. The interaction energy (E_{int}) is defined as follows:

$$E_{int}=E_{cat+SO_2}-E_{cat}-E_{SO_2} \quad (1)$$

Where, E_{cat+SO_2} is the total energy of the complex of SO₂ and the catalyst, E_{cat} is the total energy of the pristine catalyst, and E_{SO_2} is the total energy of the SO₂ molecule in the gas phase.

3. Results and discussion

3.1. Pristine catalysts

A 6×6 supercell of pure graphene was considered to build the quantum dots Pt- and Pd-doped graphene. The periodic supercell was converted to the non-periodic one, and all dangling bonds were capped by hydrogen atoms. As shown in Fig.1, Pt and Pd form a pyramidal shape, and the flat structure of the graphene is converted to a cone. This allows that the transition metals of Pt and Pd to be placed above the graphene surface, providing a better position to interact with adsorbable compounds on the catalyst's surface. The average bond lengths of Pt–C and Pd–C are 1.96 Å and 1.98 Å, respectively, while the C–C bond length is in the range of 1.41 Å to 1.45 Å.

3.2. SO₂ adsorption

Various SO₂ orientations on the Pt- and Pd-doped graphene surfaces were tested, and three configurations were positioned in local energy minima. Fig. 2 shows these local minimum configurations for both Pt- and Pd-doped graphene quantum dots.

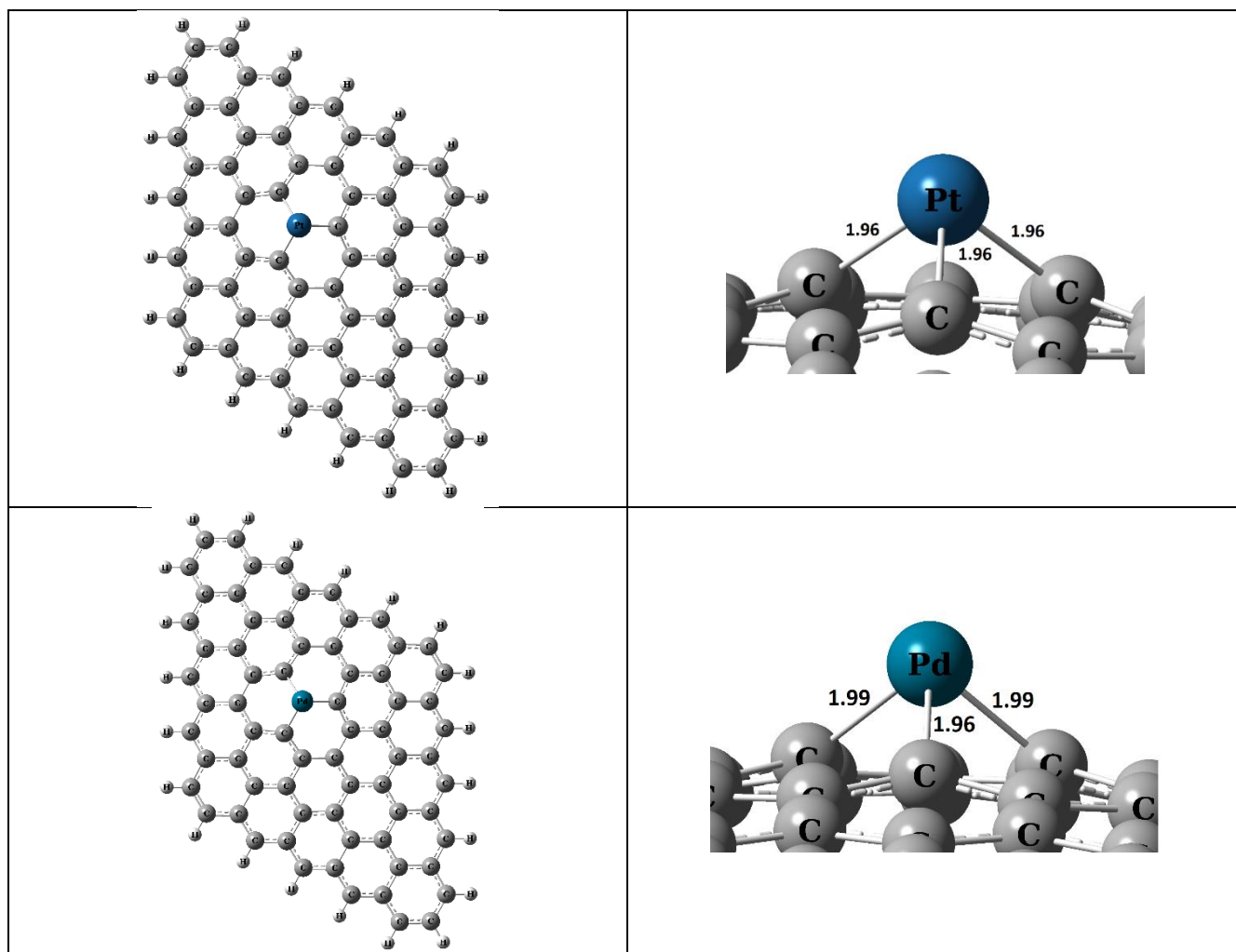


Fig. 1. The optimized structure of a Pt-doped (up) and Pd-doped (down) quantum dot graphene from side (left) and up (right) views. A 6×6 supercell was converted non-periodic and the dangling bonds were capped by hydrogen atoms.

The total energy data show that these configurations are close in energy, and their Boltzmann weights are not negligible. For both catalysts, the $\eta^1(\text{S})$ configurations are less stable compared to the $\eta^1(\text{O})\eta^1(\text{O})$ and $\eta^1(\text{S})\eta^1(\text{O})$ configurations. For Pt-doped graphene, the interaction energies for the $\eta^1(\text{O})\eta^1(\text{O})$ and $\eta^1(\text{S})\eta^1(\text{O})$ configurations are very similar, with a difference of only 0.05 eV. The $\eta^1(\text{S})\eta^1(\text{O})$ configuration is the more stable one. On the other hand, for the Pd-doped graphene quantum dot, the $\eta^1(\text{O})\eta^1(\text{O})$ configuration is the most stable one. The difference in total energies of these two configurations is approximately 0.2 eV for Pd-doped graphene.

Using a simplified version of Redhead equation with $\nu=10^{13} \text{ s}^{-1}$, it is possible to correlate the interaction energy with the desorption temperature (in Kelvin) [49]. In this simplified equation, the temperature is calculated from: $E_{\text{int}}(\text{in kJmol}^{-1})=0.25 \times T$. Therefore, the SO_2 desorption

temperatures for the Pt- and Pd-doped graphene quantum dots are 370 K and 308 K, respectively. These data show that the SO_2 adsorption on these catalysts is stable at room temperature, and it is possible to desorb SO_2 from the surfaces of the catalysts with small energy. However, it should be tested whether the SO_2 molecule dissociates at these temperatures. By calculating the barrier energy of dissociation for the SO_2 molecule, it is possible to derive the dissociation temperature using the simplified Redhead equation.

3.3. SO_2 dissociation

Fig. 3 shows the optimized configurations of reactants, transition states, and products for the first step of dissociation of SO_2 on Pt- and Pd-doped graphene quantum dots.

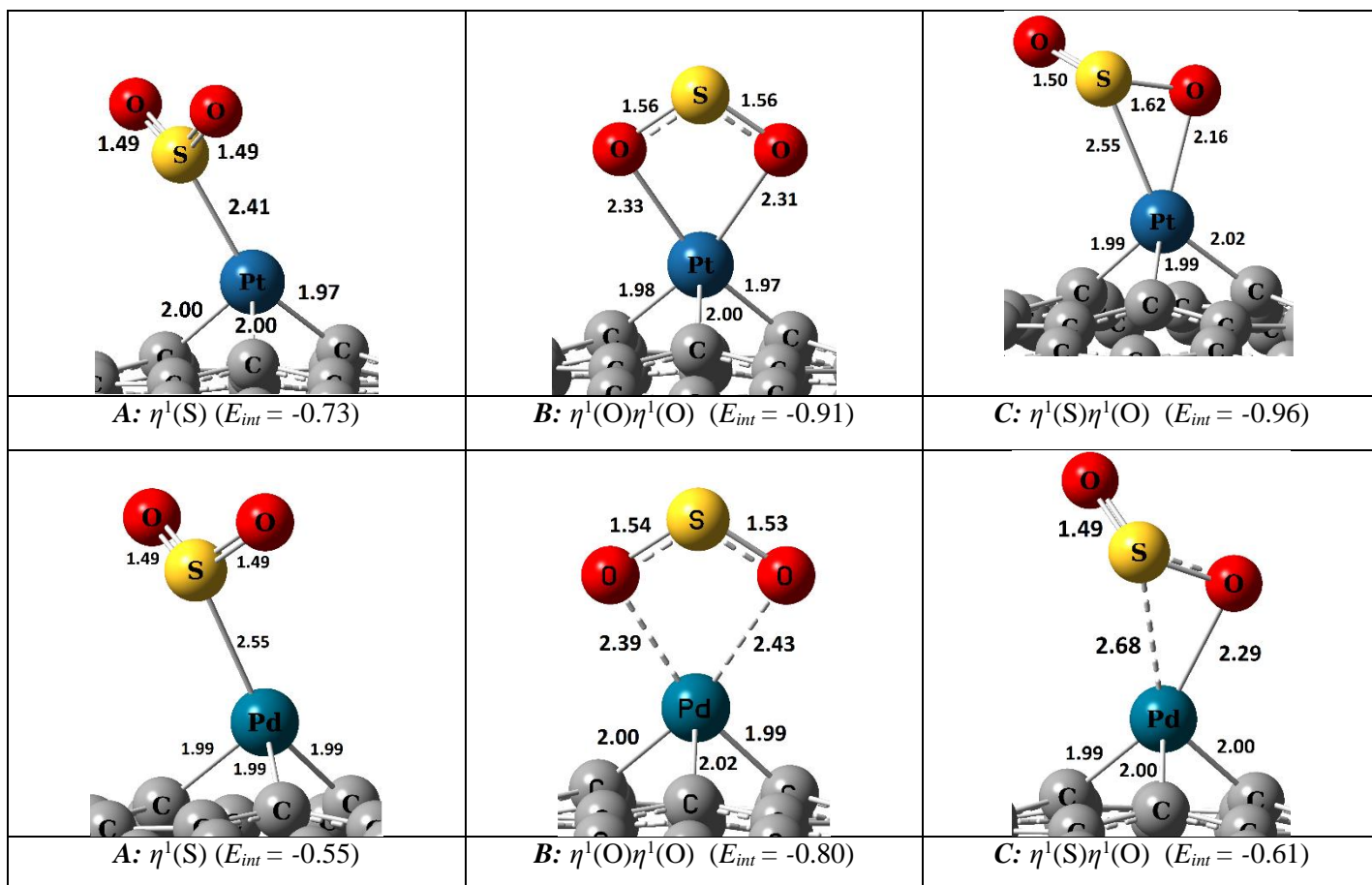


Fig. 2. Different optimized configuration of SO₂ on Pt-doped (up) and Pd-doped (down) graphene quantum dot catalyst surfaces. Pt-doped graphene prefers $\eta^1(\text{S})\eta^1(\text{O})$ configuration of SO₂ adsorption, while, on Pd-doped graphene quantum dot surface, the configuration $\eta^1(\text{O})\eta^1(\text{O})$ is the most stable one. All interaction energies are in eV.

Table 1. Barrier energies and TS location for SO₂ and SO dissociations on Pt-doped and Pd-doped graphene quantum dot catalyst surfaces. All values are in eV. Star means that the species is adsorbed on the surface of the catalysts.

No.	reaction	M	Barrier Energy	TS location
1	SO ₂ * → SO* + O*	Pt	+2.24	0.90
2	SO* → S* + O*	Pt	+2.18	0.90
3	SO ₂ * → SO* + O*	Pd	+2.95	0.89
4	SO* → S* + O*	Pd	+2.69	0.67

Table 1 shows that the TS locations for both catalysts are greater than 0.5, indicating the structures of the first TS are more similar to the products than the reactants. The separated oxygen tends to interact only with the Pt/Pd, while the separated SO interacts with both transition metal and the connected carbon atom. The barrier energies for the first step of SO₂ dissociations are 2.24 eV for Pt-doped graphene and 2.95 eV for Pd-doped graphene (see Table 1). Using the simplified Redhead equation, the corresponding dissociation temperatures of SO₂ to SO +

O are 864 K for Pt- and 1138 K for Pd-doped graphene quantum dots, which are significantly higher than the desorption temperatures required to simply desorb intact SO₂ from these catalysts. Therefore, it can be concluded that SO₂ dissociation does not occur on the surface of these doped graphene catalysts, and instead, they are good candidates for trapping SO₂ in molecular form. This is in contrast to pristine transition metal catalysts, where low SO₂ dissociation barriers lead to poisoning of the surface. On the Pt- and Pd-doped graphene catalysts, SO₂ can be

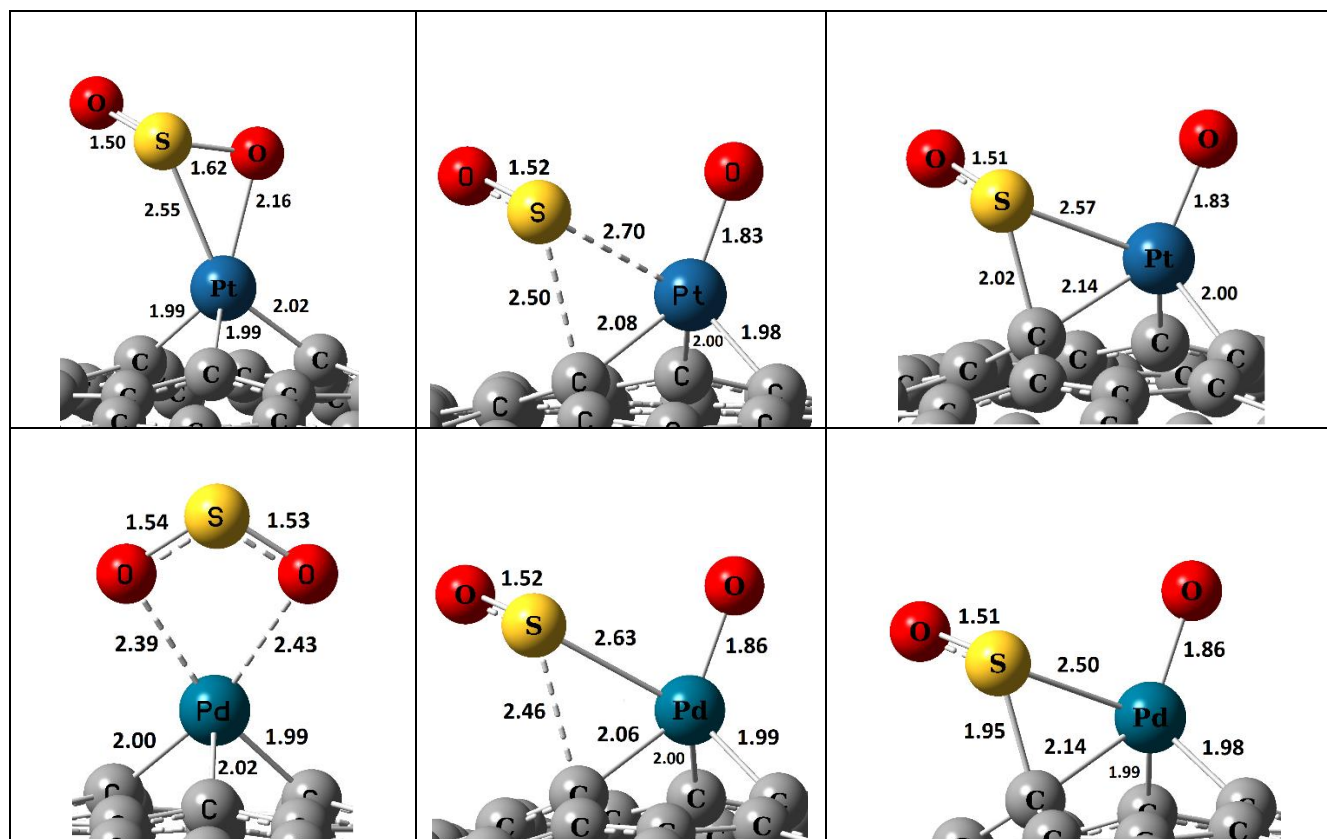


Fig. 3. Reactants (left), transition states (middle) and products (right) for SO_2 dissociation to $\text{SO} + \text{O}$ on Pt-doped (up) and Pd-doped (down) graphene quantum dot catalysts. All interaction energies are in eV.

readily adsorbed, stored, and transported without dissociating. This means that SO_2 can be simply adsorbed, reserved, and transported on the surface of Pt- and Pd-doped graphene catalysts.

We have also studied the second step of SO_2 dissociation, which is the conversion of SO to $\text{S} + \text{O}$ on the surface of both catalysts. Fig. 4 shows the optimized structure of the reactant SO , TS, and the product $\text{S} + \text{O}$ on the surfaces of Pt- and Pd-doped graphene quantum dot catalysts. Table 1 presents the locations of the TS structures and their corresponding barrier energies. Similar to the first step of SO_2 dissociation, in the second step, the locations of TS structures are above 0.5, indicating that these structures for both catalysts resemble the products. Similarly, like in the first step, the barrier energies for the second step exceed 2.0 eV, suggesting SO cannot be dissociated into $\text{S} + \text{O}$ on these catalyst surfaces.

4. Conclusion

Non-periodic density functional theory was used to investigate the adsorption and dissociation of SO_2 on the surfaces of both Pd- and Pt-doped graphene quantum dots in cluster mode. The data indicate that the adsorption energies of SO_2 on the surfaces of Pt- and Pd-doped graphene quantum dots range from -0.6 eV to -0.8 eV and -0.6 eV to -1.0 eV, respectively. However, their barrier energies (SO_2 to $\text{SO} + \text{O}$, and SO to $\text{S} + \text{O}$) exceed +2.0 eV, more than twice those on the surfaces of pristine transition metals.

Data show that these catalysts are promising catalysts for SO_2 storage and transporting by moderately adsorption/desorption energies and high barrier energy of SO_2 to S conversion. In contrast to the pristine transition metal surfaces, these high barrier energies prevent surface poisoning in the studied catalysts. So, it is suggested that the idea is developed for the periodic doped graphene, which can be more readily synthesized.

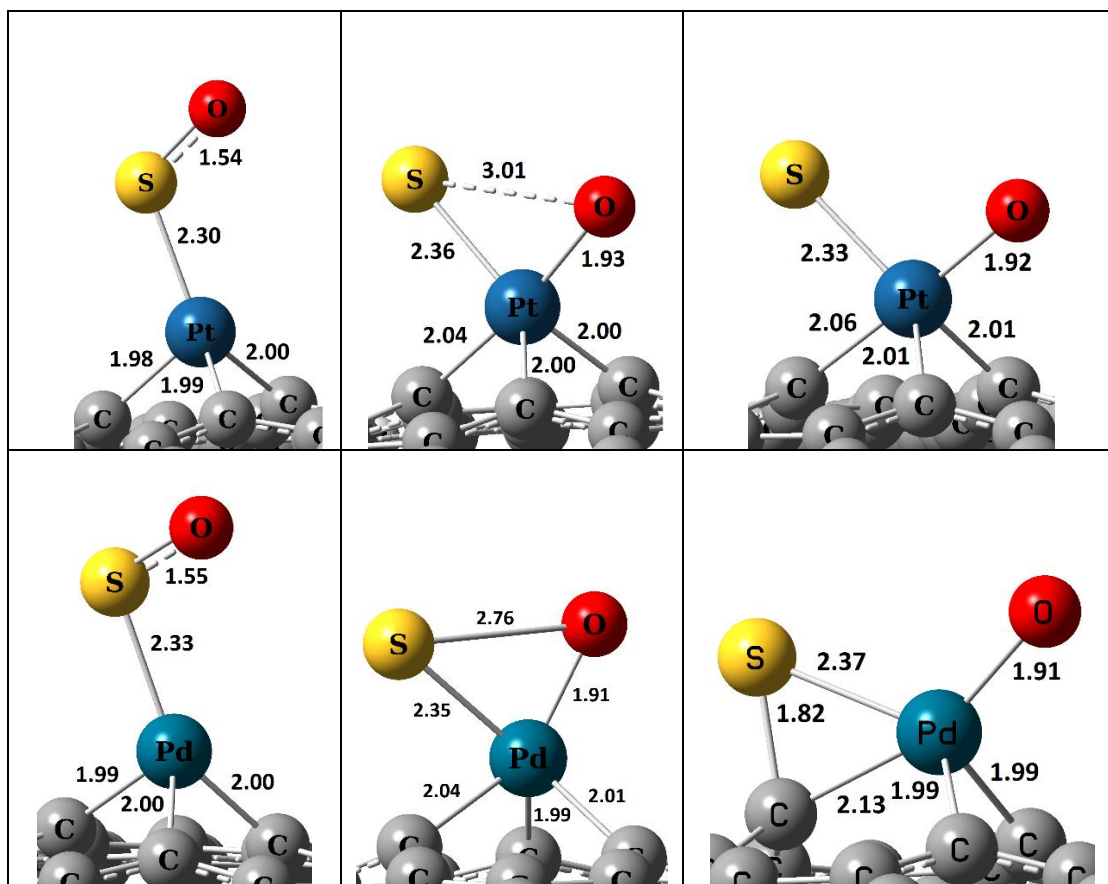


Fig. 4. Reactants (left), transition state (middle), and products of SO₂ dissociation to S + O on Pt-doped (up) and Pd-doped (down) graphene quantum dot catalysts. All interaction energies are in eV.

Acknowledgments

The authors are grateful to Ardakan and Azerbaijan State universities for their support.

References

- [1] D. Vallero, in *Fundamentals of Air Pollution (Fifth Edition)*, ed. D. Vallero, Academic Press, Boston, 2014, p. 1, <https://doi.org/10.1016/B978-0-12-401733-7.02001-6>.
- [2] L. Wilde, M. Polcik, J. Haase, B. Brena, D. Cocco, G. Comelli, G. Paolucci, Adsorption and temperature-dependent decomposition of SO₂ on Ni(110): an XPS and XAFS study, *Surf. Sci.*, 405 (1998), 215-227, [https://doi.org/10.1016/S0039-6028\(98\)00050-8](https://doi.org/10.1016/S0039-6028(98)00050-8).
- [3] G.J. Jackson, D.P. Woodruff, A.S.Y. Chan, R.G. Jones, B.C.C. Cowie, The local structure of SO₂ and SO₃ on Ni(111), *Surf. Sci.*, 577 (2005), 31-41, <https://doi.org/10.1016/j.susc.2004.12.023>.
- [4] A.R. Alemozafar, R.J. Madix, Reaction of sulfur dioxide with Ni(100) and Ni(100)-p(2x2)-O, *Surf. Sci.*, 592 (2005), 141-149, <https://doi.org/10.1016/j.susc.2005.07.003>.
- [5] A.R. Alemozafar, X.-C. Guo, R.J. Madix, Topographic nano-restructuring: sulfur dioxide adsorption on Cu(110), *Surf. Sci.*, 524 (2003), L84-L88, [https://doi.org/10.1016/S0039-6028\(02\)02539-6](https://doi.org/10.1016/S0039-6028(02)02539-6).
- [6] G.J. Jackson, S.M. Driver, D.P. Woodruff, N. Abrams, R.G. Jones, M.T. Butterfield, M.D. Crapper, B.C.C. Cowie, V. Formoso, A structural study of the interaction of SO₂ with Cu(111), *Surf. Sci.*, 459 (2000), 231-244, [https://doi.org/10.1016/S0039-6028\(00\)00497-0](https://doi.org/10.1016/S0039-6028(00)00497-0).
- [7] C.M. Pradier, P. Dubot, Adsorption and Reactivity of Sulfur Dioxide on Cu(110). Influence of Oxidation and Hydroxylation of the Surface, *J. Phys. Chem. B*, 102 (1998), 5135-5144, <https://doi.org/10.1021/jp981000c>.
- [8] T. Nakahashi, H. Hamamatsu, S. Terada, M. Sakano, F. Matsui, T. Yokoyama, Y. Kitajima, T. Ohta, Adsorption and surface reaction of SO₂ on Cu (100) studied by S K-edge XAFS and STM, *Le Journal de Physique IV*, 7 (1997), C2-679-C672-681, <https://doi.org/10.1051/jp4:1997203>.
- [9] T. Jirsak, J.A. Rodriguez, J. Hrbek, Chemistry of SO₂ on Mo(110), MoO₂/Mo(110) and Cs/Mo(110) surfaces: effects of O and Cs on the formation of SO₃ and SO₄ species, *Surf. Sci.*, 426 (1999), 319-335, [https://doi.org/10.1016/S0039-6028\(99\)00287-3](https://doi.org/10.1016/S0039-6028(99)00287-3).
- [10] T. Jirsak, J.A. Rodriguez, S. Chaturvedi, J. Hrbek, Chemistry of SO₂ on Ru(001): formation of SO₃ and SO₄, *Surf. Sci.*, 418 (1998), 8-21, [https://doi.org/10.1016/S0039-6028\(98\)00652-9](https://doi.org/10.1016/S0039-6028(98)00652-9).
- [11] M. Polčik, L. Wilde, J. Haase, B. Brena, G. Comelli, G. Paolucci, High-resolution XPS and NEXAFS study of SO₂ adsorption on Pt(111): two surface SO₂ species, *Surf. Sci.*,

- 381 (1997), L568-L572, [https://doi.org/10.1016/S0039-6028\(97\)00060-5](https://doi.org/10.1016/S0039-6028(97)00060-5).
- [12] M.L. Burke, R.J. Madix, SO₂ structure and reactivity on clean and sulfur modified Pd(100), *Surf. Sci.*, 194 (1988), 223-244, [https://doi.org/10.1016/0039-6028\(94\)91257-2](https://doi.org/10.1016/0039-6028(94)91257-2).
- [13] R. Kumar, Study of conduction mechanism in swift heavy ion irradiated reduced graphene oxide samples and its applications towards low level detection of SO₂ at room temperature, *Diamond Relat. Mater.*, 144 (2024), 111057, <https://doi.org/10.1016/j.diamond.2024.111057>.
- [14] A. Shokuhi Rad, D. Zareyee, Adsorption properties of SO₂ and O₃ molecules on Pt-decorated graphene: A theoretical study, *Vacuum*, 130 (2016), 113-118, <https://doi.org/10.1016/j.vacuum.2016.05.009>.
- [15] Q. Luo, S. Yin, X. Sun, Y. Tang, Z. Feng, X. Dai, Density functional theory study on the adsorption properties of SO₂ gas on graphene, N, Ti, and N-Ti doped graphene, *Micro and Nanostructures*, 171 (2022), 207401, <https://doi.org/10.1016/j.micrna.2022.207401>.
- [16] X. Yan, T. Shen, X. Liu, C. Liu, A. Gong, Transition metal (Co, Ti) decorated graphene monolayer and their adsorption properties towards SO₂: First-principle calculation, *Solid State Commun.*, 369 (2023), 115196, <https://doi.org/10.1016/j.ssc.2023.115196>.
- [17] H. Louis, K. Chukwuemeka, E.C. Agwamba, H.Y. Abdullah, A.M.S. Pembere, Molecular simulation of Cu, Ag, and Au-decorated Si-doped graphene quantum dots (Si@QD) nanostructured as sensors for SO₂ trapping, *J. Mol. Graphics Modell.*, 124 (2023), 108551, <https://doi.org/10.1016/j.jmkgm.2023.108551>.
- [18] X. Zhang, M. Hou, W. Cen, W. Jiao, A DFT study of H₂S, H₂O, SO₂ and CH₄ Adsorption Behavior on Graphene Surface Decorated with Alkaline Earth Metals, *Surf. Sci.*, 726 (2022), 122178, <https://doi.org/10.1016/j.susc.2022.122178>.
- [19] P. Xu, Y. Gui, X. Chen, A DFT study of adsorption properties of SO₂, SOF₂, and SO₂F₂ on ZnO/CuO doped graphene, *Diamond Relat. Mater.*, 126 (2022), 109103, <https://doi.org/10.1016/j.diamond.2022.109103>.
- [20] E. Salih, A.I. Ayesh, Sensitive SO₂ gas sensor utilizing Pt-doped graphene nanoribbon: First principles investigation, *Mater. Chem. Phys.*, 267 (2021), 124695, <https://doi.org/10.1016/j.matchemphys.2021.124695>.
- [21] R.F. de Menezes, F. Pirani, C. Coletti, L.G.M. de Macedo, R. Gargano, Functionalized graphene-based Quantum Dots: Promising adsorbents for CO, NO₂, SO₂, and NH₃ Pollutant Gases, *Materials Today Communications*, 31 (2022), 103426, <https://doi.org/10.1016/j.mtcomm.2022.103426>.
- [22] Z. Zhang, B. Liang, Y. Chi, Y. Jiang, J. Song, Y. Guo, Adsorption mechanism of SO₂ on vacancy-defected graphene and Ti doped graphene: A DFT study, *Superlattices Microstruct.*, 159 (2021), 107036, <https://doi.org/10.1016/j.spmi.2021.107036>.
- [23] E. Salih, A.I. Ayesh, CO, CO₂, and SO₂ detection based on functionalized graphene nanoribbons: First principles study, *Physica E: Low-dimensional Systems and Nanostructures*, 123 (2020), 114220, <https://doi.org/10.1016/j.physe.2020.114220>.
- [24] X. Gao, Q. Zhou, J. Wang, L. Xu, W. Zeng, Adsorption of SO₂ molecule on Ni-doped and Pd-doped graphene based on first-principle study, *Appl. Surf. Sci.*, 517 (2020), 146180, <https://doi.org/10.1016/j.apsusc.2020.146180>.
- [25] D. Cortés-Arriagada, N. Villegas-Escobar, D.E. Ortega, Fe-doped graphene nanosheet as an adsorption platform of harmful gas molecules (CO, CO₂, SO₂ and H₂S), and the co-adsorption in O₂ environments, *Appl. Surf. Sci.*, 427 (2018), 227-236, <https://doi.org/10.1016/j.apsusc.2017.08.216>.
- [26] D. Bijani, R. Ghiasi, S. Baniyaghoob, DFT investigation of stability, electronic and optical properties of coordination of C₂₀ corannulene to Fe(CO)₄, *Inorg. Chem. Commun.*, 153 (2023), 110793, <https://doi.org/10.1016/j.inoche.2023.110793>.
- [27] S. Shayanmehr, R. Ghiasi, B. Mirza, B. Mohtat, HYDROGEN ADSORPTION AND STORAGE ON PALLADIUM-FUNCTIONALIZED C₂₀ BOWL AND C₂₀H₁₀ BOWL MOLECULE INCLUDING HYDROGEN SATURATION, *J. Struct. Chem.*, 63 (2022), 1399-1408, 10.1134/S0022476622090037.
- [28] A. Hedieh, R. Ghiasi, M. Yousefi, S. Baniyaghoob, Electronic, Structural, and Optical Properties of Fe(CO)₄[X₁₂Y₁₂] (X = B or Al, Y = N or P) Complexes: A Computational Investigation, *Russian Journal of Inorganic Chemistry*, 68 (2023), 1065-1076, 10.1134/S0036023623600338.
- [29] A. Amiri, R. Ghiasi, K. Zare, R. Fazaeli, Interaction between Phosgene and B₁₂N₁₂ Nano-Cluster: A Computational Investigation, *Russian Journal of Physical Chemistry A*, 95 (2021), S323-S330, 10.1134/S0036024421150036.
- [30] E. Vessally, M. Hosseinali, M.R. Poor Heravi, B. Mohammadi, DFT study of the adsorption of simple organic sulfur gases on g-C₃N₄; periodic and non-periodic approaches, *Journal of Sulfur Chemistry* 1-18, 10.1080/17415993.2023.2209687.
- [31] F. Behmagham, E. Vessally, B. Massoumi, A. Hosseinian, L. Edjlali, A computational study on the SO₂ adsorption by the pristine, Al, and Si doped BN nanosheets, *Superlattices Microstruct.*, 100 (2016), 350-357, <https://doi.org/10.1016/j.spmi.2016.09.040>.
- [32] S. Kamalinahad, E. Vessally, Assessing the sensing performance of a decorated B₂₂ nanocluster for SO₂ gas detection: an in silico study, *Journal of Sulfur Chemistry*, 45 (2024), 24-41, <https://doi.org/10.1080/17415993.2023.2272008>.
- [33] E. Vessally, M.R. Ilghami, M. Abbasian, Investigation the Capability of Doped Graphene Nanostructure in Magnesium and Barium Batteries with Quantum Calculations, *Chemical Research and Technology*, 1 (2024), 10.2234/chemrestec.2024.436837.1007.
- [34] R. Behjatmanesh-Ardakani, T.T. Magkoev, SO₂ adsorption and its direct proportional dissociation on the Cu(100), Cu(110), and Cu(111) surfaces: a periodic DFT

- study, *Chemical Review and Letters* (2024), 10.22034/crl.2024.467740.1380.
- [35] R. Behjatmanesh-Ardakani, Theoretical Insights into Band Gap Tuning Through Cu Doping and Ga Vacancy in GaSe Monolayer: A First-Principles Perspective, *J. Electron. Mater.*, 53 (2024), 2398-2409, 10.1007/s11664-024-10977-2.
- [36] S. Majedi, H.G. Rauf, M. Boustanbakhsh, DFT study on sensing possibility of the pristine and Al- and Ga-embedded B12N12 nanostructures toward hydrazine and hydrogen peroxide and their analogues, *Chemical Review and Letters*, 2 (2019), 176-186, 10.22034/crl.2020.216625.1032.
- [37] A.A. Al-Sattar Dawood, A.H. Abdul Hussein, K.R. Al-Shami, B. Azizi, R. Thabit, H. M. H, R.O. kareem, Electronic and Magnetic Structure of Monolayer MnAs (111): A case study by DFT, *Chemical Review and Letters*, 7 (2024), 373-379, 10.22034/crl.2024.448436.1312.
- [38] F. Alimohammadi, G. Rezanejade Bardajee, A. Monfared, The sensing behavior of MgO nanotube to thiopropamine drug via DFT investigation, *Chemical Review and Letters*, 7 (2024), 513-521, 10.22034/crl.2024.457011.1335.
- [39] B. Hammer, L.B. Hansen, J.K. Nørskov, Improved adsorption energetics within density-functional theory using revised Perdew-Burke-Ernzerhof functionals, *Phys. Rev. B*, 59 (1999), 7413-7421, <https://doi.org/10.1103/PhysRevB.59.7413>.
- [40] Z.-Y. Qiu, J.-S. Dang, Mechanistic studies on defective hBN-supported metal-nonmetal synergistic catalysis for urea electrosynthesis, *Appl. Surf. Sci.*, 679 (2025), 161230, <https://doi.org/10.1016/j.apsusc.2024.161230>.
- [41] R. Behjatmanesh-Ardakani, A. Heydari, Molecular and dissociative adsorption of tetrachlorodibenzodioxin on M-doped graphenes (M = B, Al, N, P): pure DFT and DFT + VdW calculations, *J. Mol. Model.*, 26 (2020), 164, 10.1007/s00894-020-04387-4.
- [42] R. Behjatmanesh-Ardakani, E.M. Bahalkeh, V. Moeini, A mechanistic periodic DFT study of CH, CO, and OH dissociations in methanol: M-doped carbon nanotubes (M = Pt, B, Al, N, P) versus Pt(100), Pt(110) and Pt(111) surfaces, *Mol. Catal.*, 512 (2021), 111781, <https://doi.org/10.1016/j.mcat.2021.111781>.
- [43] R. Behjatmanesh-Ardakani, Periodic hybrid-DFT study on the N-doped TiO₂ (001) nanotubes as solar water splitting catalysts: A comparison with the rutile and anatase bulk phases, *Int. J. Hydrogen Energ.*, 48 (2023), 35584-35598, <https://doi.org/10.1016/j.ijhydene.2023.05.352>.
- [44] R. Behjatmanesh-Ardakani, A. Moradzadeh, Dual surface doping of Co+N in the anatase TiO₂(100) for water splitting process, *Chemical Review and Letters*, 7 (2024), 17-19, 10.22034/crl.2024.435210.1278.
- [45] B. Delley, Hardness conserving semilocal pseudopotentials, *Phys. Rev. B*, 66 (2002), 155125, <https://doi.org/10.1103/PhysRevB.66.155125>.
- [46] B. Delley, An all-electron numerical method for solving the local density functional for polyatomic molecules, *J. Chem. Phys.*, 92 (1990), 508-517, <https://doi.org/10.1063/1.458452>.
- [47] B. Delley, From molecules to solids with the DMol³ approach, *J. Chem. Phys.*, 113 (2000), 7756-7764, <https://doi.org/10.1063/1.1316015>.
- [48] R. Jiang, W. Guo, M. Li, H. Zhu, J. Li, L. Zhao, D. Fu, H. Shan, Density Functional Study of the Reaction of SO₂ on Ir(111), *J. Phys. Chem. C*, 113 (2009), 18223-18232, <https://doi.org/10.1021/jp9054999>.
- [49] P.A. Redhead, Thermal desorption of gases, *Vacuum*, 12 (1962), 203-211, [https://doi.org/10.1016/0042-207X\(62\)90978-8](https://doi.org/10.1016/0042-207X(62)90978-8).